16th European Conference on Fracture, Alexandroupolis, GREECE 2006

THREE-DIMENSIONAL EXPERIMENTAL AND NUMERICAL SIFS AND CRACK GROWTH

D. M. Constantinescu[1], B. Bocăneală[1], L. Marşavina[2]
[1]Department of Strength of Materials, University “Politehnica” of Bucharest,
Splaiul Independenței nr. 313, Bucureşti, ROMANIA
[2]Department of Strength of Materials, University “Politehnica” of Timişoara,
B-dul Mihai Viteazul nr.1, Timişoara, ROMANIA
dancon1@form.resist.pub.ro, bbocaneala@form.resist.pub.ro, msvina@mec.utt.ro

ABSTRACT

Experimental evidence on three-dimensional crack propagation is needed for a better understanding of the local mechanisms around the crack front in a complex geometry. The experimental observations of crack propagation and turning processes suggest that the role of the shear modes is important in the initial stages of growth. A three-dimensional boundary element analysis is used to compare the SIF values and predict crack growth as trying to assess the efficiency of a numerical simulation by using a cheaper but also reliable procedure.

General considerations

The desire to establish a three-dimensional (3D) framework for use in analyzing problems of stable mixed-mode crack propagation has received lately a considerable attention. The study of predicting crack paths under the most general possible hypotheses (three dimensions, arbitrary geometry of the body and of the crack, arbitrary loading) is an ambitious objective. In some approaches the perturbation of the crack will result from addition of some small extension as in the works of Rice [1,2], Gao and Rice [3-5], Gao [6] and Nazarov [7], and the prediction of the crack path will result from combinations of asymptotic expressions of the stress intensity factors (SIFs) for infinitesimal crack extension lengths and some appropriate criterion. Recently, Leblond [8] and Leblond, Lazarus and Mouchrif [9] established formulae which specify the general functional form of the successive terms of the expansions of the SIFs along the front of the extended crack and, as they underline, the formulation of the propagation criterion is an open problem only in the presence of mode III. Therefore, in a mode I+II situation, the widely accepted “principle of local symmetry” of Goldstein and Salganik [10] receives a general recognition. In fact, for the two-dimensional problem, Cotterell and Rice [11] presented an analysis for slightly curved or kinked cracks and accounted for the role of mode II in crack turning. Also Rubenstein [12], in analyzing test results, concluded that sharp kinks likely occur only in very brittle materials and that, more commonly, the change in direction during the crack growth is more of a gradual turning than a kink. More recently the influence of crack surface and crack front curvature upon the various forms of the domain independent *F*-integral is discussed by Eriksson [13] for the three-dimensional case. In numerical experiments the FRANC3D code uses new concepts with a model that allows for the implementation of 3D crack growth mechanics [14] with the support of both finite and boundary elements. New developments consider the crack discontinuity as a Heaviside step function and branch functions are introduced for elements containing the crack front [15,16]. This enables the construction of the three-dimensional near-tip asymptotic field even when the crack is curved or kinked at the tip; the need for an explicit surface model of the crack is also eliminated as this is described by nodal data and the element topology doesn’t need to conform to the surfaces of the crack, whose front can pass through an element. On the whole one can get rid of the tedious remeshing methods as the crack can be altered or grown by changing the level sets (discontinuous partition of unity), and this is useful for an engineering analysis of a structure with multiple cracks.

Keeping in mind such beneficial developments, one should emphasize that for a specific geometry and loading we may obtain various experimental crack paths which are dependent on the local position of the initial crack, as any deviation from “symmetry” influences the future crack trajectory. However, to perform experiments is expensive, and numerical 3D simulations to calculate SIFs and study crack propagation are very appealing if proved to be efficient. Our examples try to assess how reliable can be the numerical experiment when cracks of different locations appear in a complex geometry.

Model configuration and experimental procedure

The geometry of the model studied here is shown in Fig. 1 and represents a motor grain configuration [17]. A model contained two starter cracks, a *symmetric* and an *off-axis* crack separated by an uncracked fin to avoid any

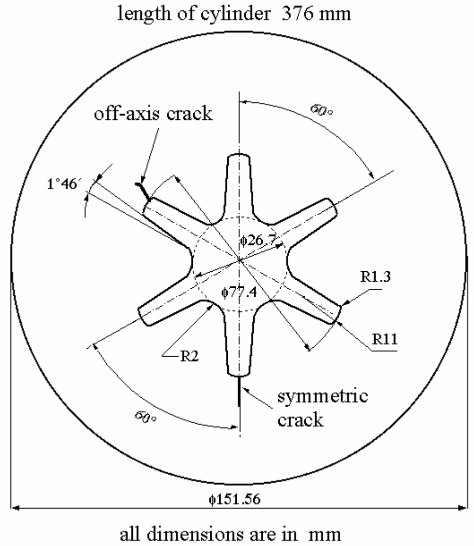

Figure 1. Tested model geometry.

interference. After inserting the starter cracks by striking a shaft with a blade at the end held normal to the inner fin surface, the models were capped with RTV rubber caps which were glued with PMC-1 adhesive and were subjected to the stress freezing cycle under internal pressure. The cracks were grown under internal pressure above critical temperature to desired size, after which the pressure was dropped to about 0,04-0,05 MPa and stress freezing was completed. After cooling, thin slices (around 1 mm thickness) were removed normal to the crack front and analyzed at maximum crack depth and in certain locations along the crack front, finally obtaining the values of the normalized stress intensity factors by using a two parameter algorithm valid within the linear elastic fracture mechanics (LEFM) constrains [18]. Thus optical data (isochromatic fringes) can be converted into mode I and mode II SIFs, if the last one exists.

Crack growth behaviour

Studies of 11 tests on the motor grain geometry covered cracks of projected *a/c* values (crack depth/half length of crack in fin tip surface) of 0,5 to 0,9 and *a/t* values from 0,2 to 0,6 (*t* = 37,08 mm is the cylinder wall thickness at fin tip). It appears that both SIF values and crack geometry during growth are quite variable due to shear modes for the off-axis inclined cracks. On the other hand, the symmetric cracks situated on the fin axis are quite predictable in their growth, as they tended to grow much more readily than the off-axis crack, always in the plane of the fin axis. It was found that the substantial delay in crack growth for the inclined cracks is also due to some initial misalignment of the blade with respect to the normal to the fin surface that is corrected by the turning of the crack as it grows and eliminates the shear modes.

All cracks on the fin axis remained in the plane of the axis of symmetry and grew as semi-elliptic cracks. If the cracks were straight-in parallel to the fin axis but located at the coalescence of the two radii of 1,3 mm and 11 mm (Fig. 1), a slight initial crack plane misalignment is again possible due to the position of the blade or due to its bending after striking it, but the crack grows quickly by regaining its symmetry, parallel to the fin axis.

A more complex crack growth was produced using the off-axis inclined orientation of the blade and shown in Fig. 2 [19]. A plan view with the crack in Model 4 shows an essentially semi-elliptic starter crack which enters the model normal to the fin surface (FS).

When internal pressure is applied the crack turns on a curved path (note path of mid-point in section S-S), and after this limited amount of growth some Mode II as well as Mode I remained. Presumably, with further extension, the crack will straighten out and eliminate Mode II.

The second type, exhibited by Model 8, revealed a much more complex crack surface. Although the starter crack was again a semi-ellipse, during the growth and the turning process of the crack appeared radial river markings, suggesting the presence of mode III along with modes I and II. The shape was complicated with “ears” along the fin surface, were the growth extends initially more than at center-point, probably related to the river markings. As shown in the photo of Model 8, a dimple or slowing of crack growth occurs were river marks are, and as crack grows the separation of the fracture surface (river marks indicated by different light reflections in photo) fades out together with the elimination of mode III. During growth the curved 3-D crack surface gradually tends to become plane. When this picture was taken no mode II was present (notice the straight path at center-point), and it can be assumed that, with more growth, the crack would regain its nearly semi-elliptic shape.

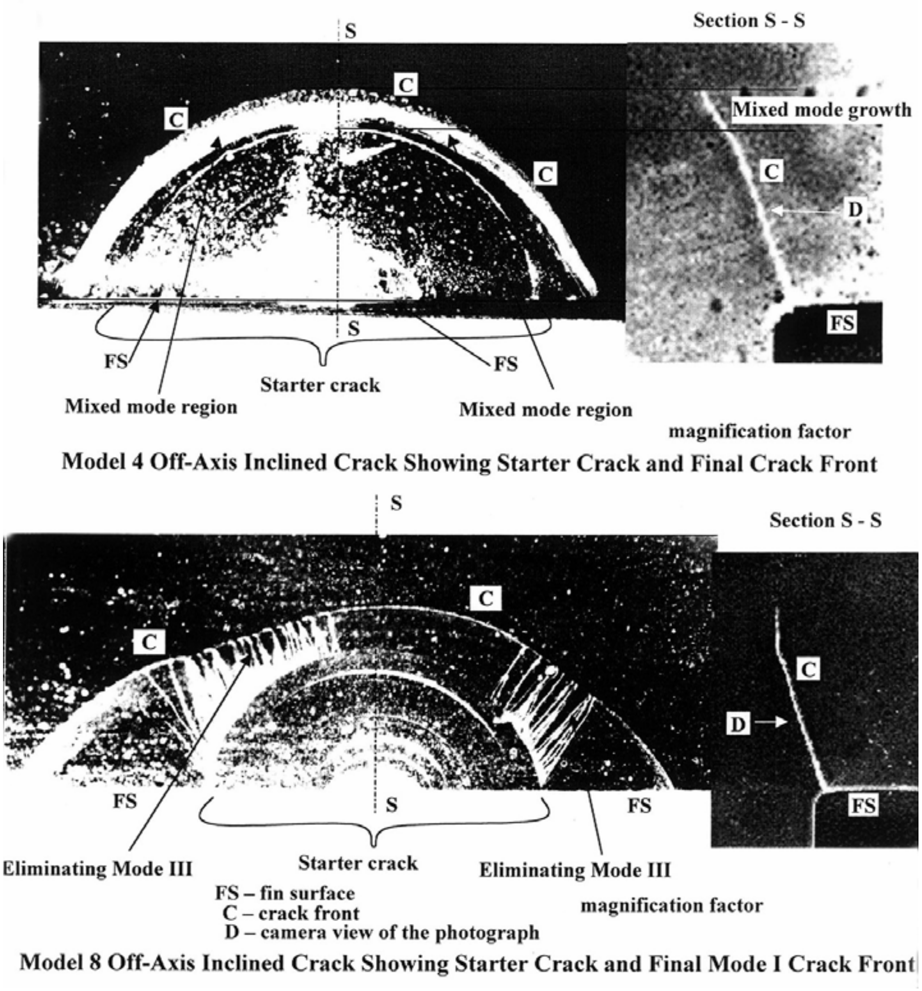

Figure 2. Projected crack profiles and path of center-point [19].

Three-dimensional numerical simulations of crack growth

A FRANC2D/L plane-strain finite element analysis was initially performed on half model using triangular 6-node elements. The mesh had 988 elements with 2153 nodes. A refined mesh was used around the fins, which behave in fact like notches, introducing stress concentration at their base. The material constants used in the analysis were the same as of the photoelastic stress frozen material. The initial numerical study done by Marşavina and Constantinescu [20] had the purpose to find the SIFs versus crack length for three different configurations: symmetric crack, off-axis straight-in crack and off-axis inclined crack. The remeshing by delete and fill algorithm was used, as established by Wawrzynek and Ingraffea [21], which requires: to delete a group of elements in a region around the crack tip, then the crack is extended into this region, and singular elements are placed around the crack tip. The stress intensity factors were obtained using the Modified Crack Closure Integral method. A study of cracks propagation was carried on. The numerical prediction of the direction of crack trajectory was based on the maximum principal stress theory developed by Erdogan and Sih [22].

FRANC3D [14] is a work-station based FRacture ANalysis Code for simulating arbitrary non-planar 3D crack growth that has been under development since 1987. OSM (Object Solid Modeler) is a pre-processor to FRANC3D for building the initial geometric model. FRANC3D provides a mechanism for representing the geometry and topology of 3D structures with arbitrary non-planar cracks, along with functionality for: 1) meshing the structure, 2) attaching boundary conditions at the geometry level and allowing the mesh to inherit these values, and 3) modifying the geometry to allow crack growth, but with only local remeshing required during crack growth. The simulation process is controlled by the user through a graphical user-interface, which includes windows for the display of the 3D structure and a menu and dialog-box system for interacting with the program. FRANC3D is not tied to a particular numerical analysis scheme or program, and is able to create either surface or volume meshes. Consequently, any 3D boundary or finite element program, capable of handling arbitrary crack geometries, could be used to determine the structural response.

For obtaining the solution, in all the simulations, boundary elements were used. The propagation was done in steps, after each step the new front points of the crack were calculated and the crack was propagated with the calculated amount. Two parameters influence crack growth, the "*maximum extension (ME)*" and "*b*" which is in essence a ratio between Δa and Δc. The maximum extension parameter is a correlation factor and does not influence directly the extension of the crack, this meaning that if the value of this parameter is 1, the maximum extension of the crack is not 1 but less. In our simulation this parameter was varied from 0.5 to 5 and range of results were obtained. The "*b*" parameter influence the crack in the following way: if "*b*" is higher the crack propagates more on the surface and less in depth, in all of our simulations this parameter was kept constant at a value of 1. Maximum extension and "*b*" do not influence the value of the SIFs directly, by this understanding that if the crack has another shape (influenced by "*ME*" and "*b*") and the propagation is continued, the values of the SIFs will be different.

For the beginning a symmetric crack in half of the motor grain geometry is meshed with boundary elements as shown in Fig. 3; the model had around 900 elements and the SIFs were calculated in 24 points around the crack front. The model gave good results and gave us come confidence. Three types of symmetric cracks were propagated in this way, with different propagation steps and loading conditions.

The third and last step from this numerical prediction was to construct the full model geometry and analyze the three dimensional effects. In this case two initial cracks were considered in symmetric and opposite locations and their propagation was studied by applying or not the internal pressure on the crack flanks; of course additional pressure called further "crack loading" – which in reality appears – will open more the crack and increase the normalized SIF values. Another loading which appeared in the experiment was due to a compressive axial force of almost 89 N which was applied as a dead weigh on the top of the specimen (supported at the other end) in order to avoid any movement when internal pressure is applied. In a further plot this is labeled as "side loading".

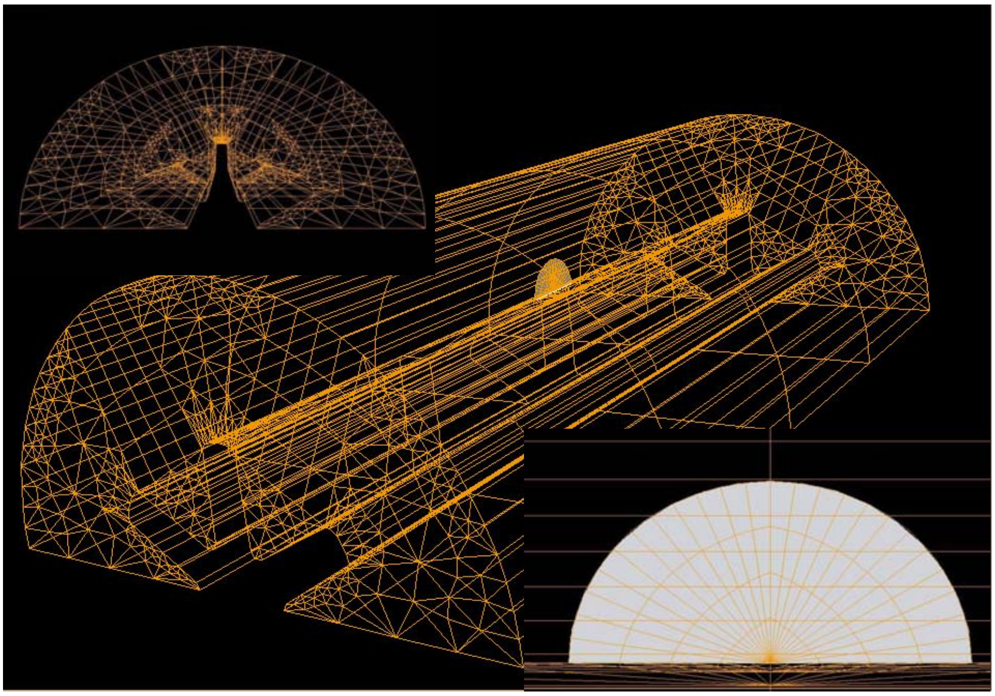

Figure 3. Half of the model meshed with boundary elements and a symmetric crack.

Our aim was to construct a *generic symmetric crack* called also *theoretical crack* with different *a/t* ratios and compare the 3D results with the experimental ones, and with those obtained from a 2D analysis by using FRANC2D/L. Different boundary conditions were applied. In Fig. 4 is presented the whole model with two cracks of same initial size before propagation, and after the propagation in 13 consecutive steps. The crack grows more if "crack loading" exists, and further extended if "side loading" is also present.

Due to global and local symmetry conditions the crack trajectory is not influenced by the loading conditions. So, the so-called symmetric crack will propagate without any change of direction, along the axis of symmetry of the fin. In the experiment we also noticed that such a crack grows more readily, that is easier, as no imperfections or un-symmetries may obstruct the free development of a crack.

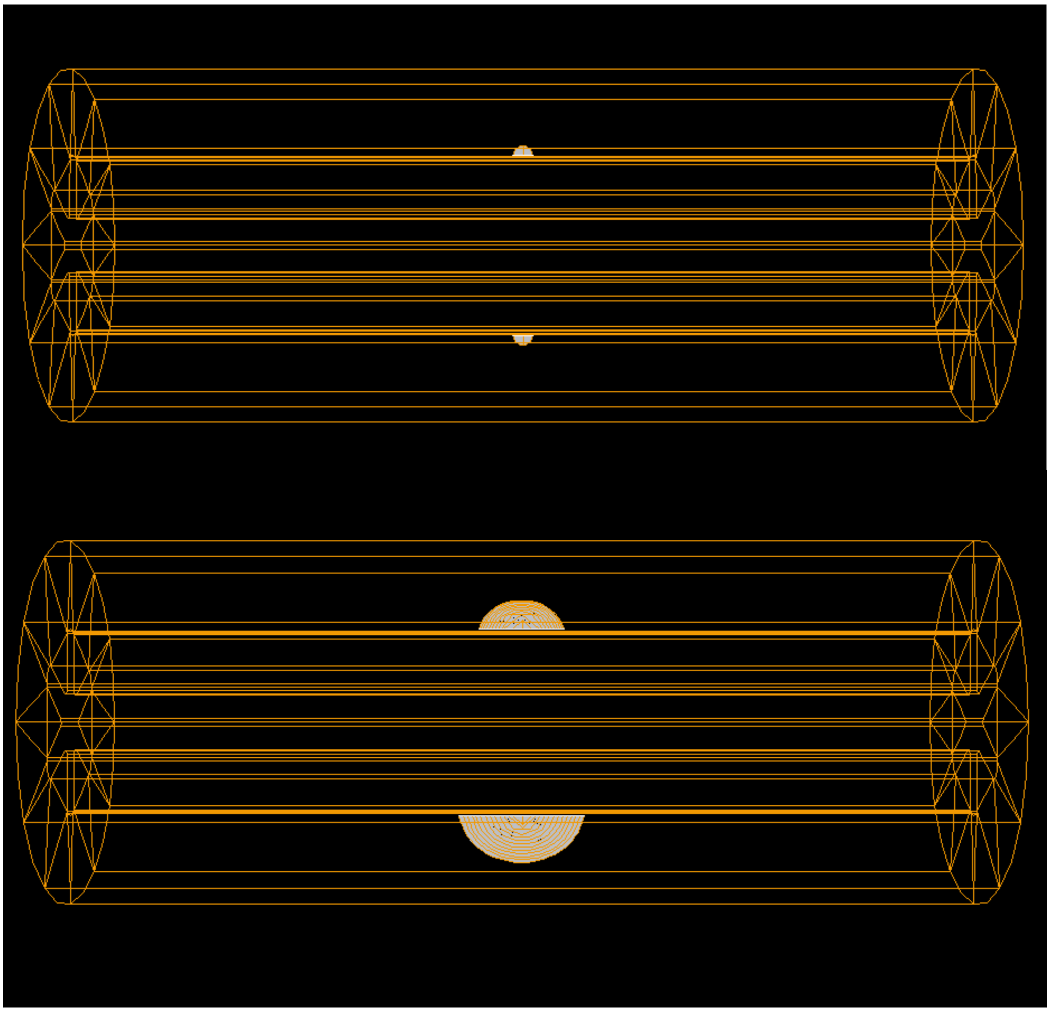

Figure 4. Full model with two symmetric cracks, before and after the propagation due to different loading conditions.

Numerical SIFs obtained with three-dimensional simulations

Out of the 11 experimental tests on the motor grain geometry only three symmetric cracks gave us Mode I normalized SIFs. Another crack penetrated through the wall thickness. To obtain normalized SIFs we used the equation $F_i = K_i \sqrt{Q} / p_{sf} \sqrt{\pi a}$, i = 1, 2 (for Mode I or Mode II) at maximum depth in the middle slice or close to the fin surface – we chose a 20 degrees angle. In this equation we have: $\sqrt{Q}$ = approximation of elliptic integral of second kind with $Q = 1 + 1.464(a/c)^{1.65}$ $a/c \le 1$; p_{sf} = stress freezing pressure used in the experiment. All flaws were characterized as semi-elliptic flaws of depth a and length $2c$. However, we should emphasize that off-axis cracks were neither perfectly semi-elliptic nor planar.

Same normalization procedure is used for obtaining numerical SIFs. In Fig. 5 is plotted the variation of SIFs obtained from a 2D analysis with FRANC2D/L. The experimentally obtained values of SIFs (for *a/t* between 0.26 and 0.4) in the middle slice and in the 20 degrees slice are situated bellow this curve, respectively coinciding with it. From the 3D analyses on the full model the cases of "crack loading" and "side loading" are imposes separately or together. Only values for the middle slice, at 90 degrees are presented in Fig. 5. Clearly "crack loading" increases significantly the normalized SIFs. The "side loading" – compressive axial force – has a small effect which increases SIFs if added to "crack loading". This effect is somehow surprising. However, experimental SIFs are in agreement with the numerical ones when there is no "crack loading", that is no internal pressure is applied on the crack surfaces.

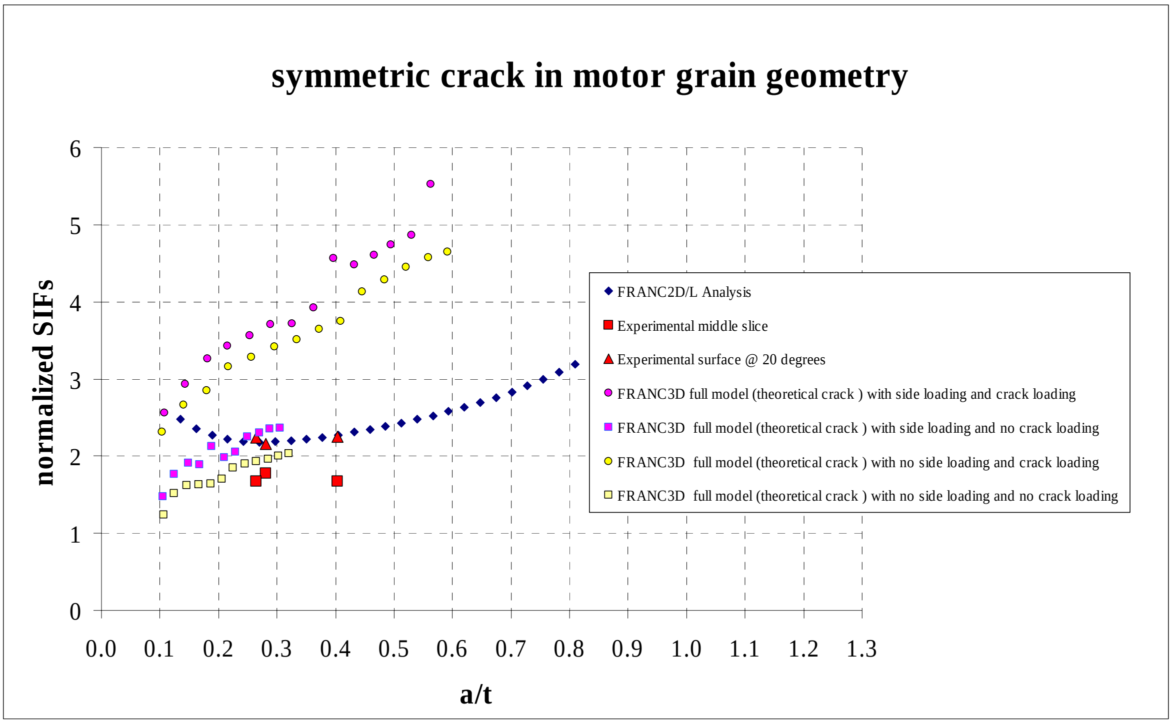

Figure 5. Numerical and experimental normalized SIFs for the complex geometry.

For an off-axis straight-in crack parallel to the fin axis or an inclined off-axis crack as normal to the fin surface the propagation of the crack is done with some difficulties and in some steps the crack propagation is stopped due to some error; only a manual remeshing was possible as to continue with the analysis. This one is very tedious and time consuming. The obtained values of normalized SIFs will be reported somewhere else.

Conclusions

Experimentally obtained normalized SIFs for a symmetric crack are almost constant for moderate deep cracks (for *a/t* between 0.26 and 0.4) having a higher value closer to the fin surface. These results are in a good agreement with the numerical 3D SIFs if there is no “crack loading”. Surprisingly, the 2D plane strain condition (obtained with FRANC2D/L) gives an upper limit of numerical SIFs, being conservative, at least for $a/t < 0.3$.

When imposing in the numerical simulation a “crack loading” of the crack surfaces the normalized SIFs increase significantly, and the increase of the crack to depth ratio *a/t* leads to increased SIFs. This tendency was not confirmed by the experimental results for the off-axis straight-in cracks. On the contrary, a negative gradient of SIFs was found.

Acknowledgement

Dan Mihai Constantinescu acknowledges the support of the above experimental studies under P.0. #RPO10230 with ERC Inc. through Air Force Research Laboratory and many useful discussions with Professor C.W. Smith. The numerical simulations were done by Bogdan Bocăneală as part of his diploma thesis defended to become a mechanical engineer.

References

1. Rice, J.R., “First-order variation in elastic fields due to variation in location of a planar front,” ASME Journal of Applied Mechanics, **52**, 571-579, 1985.
2. Rice, J.R., “Weight function theory for three-dimensional elastic crack analysis,” In R.P. Wei and R.P. Gangloff, editors, Fracture Mechanics: Perspectives and Directions (Twentieth Symposium), ASTM STP 1020, 29-57, American Society for Metals, Philadelphia, 1989.
3. Gao, H. and Rice, J.R., “Shear stress intensity factors for a planar crack with slightly curved front,” ASME Journal of Applied Mechanics, **53**, 774-778, 1986.
4. Gao, H. and Rice, J.R., “Somewhat circular tensile cracks,” International Journal of Fracture, **33**, pp. 155-174, 1987.

5. Gao, H. and Rice, J.R., "Nearly circular connections of elastic half spaces," ASME Journal of Applied Mechanics, **54**, pp. 627-634, 1987.
6. Gao, H., "Nearly circular shear mode cracks," International Journal of Solids and Structures, **24**, pp. 177-193, (1988).
7. Nazarov, S.A. - Derivation of variational inequality for the shape of the small increment of a mode I crack," Mechanics of Solids, **24**, pp. 145-152, 1989.
8. Leblond, J.B., "Crack paths in three-dimensional elastic solids. I: two-term expansion of the stress intensity factors – application to crack path stability in hydraulic fracturing," International Journal of Solids and Structures, **36**, 79-103, 1999.
9. Leblond, J.B., Lazarus, V. and Mouchrif, S., "Crack paths in three-dimensional elastic solids. I: three-term expansion of the stress intensity factors – applications and perspectives," International Journal of Solids and Structures, **36**, pp. 105-142, 1999.
10. Goldstein, R.V. and Salganik, R.L., "Brittle fracture of solids with arbitrary cracks," International Journal of Fracture, **10**, 507-523, 1974.
11. Cotterell, B. and Rice, J.R., "Slightly curved or kinked cracks," International Journal of Fracture, **16**, 155-169, 1980.
12. Rubenstein, A., "Mechanics of crack path formation," International Journal of Fracture, **47**, 291-305, 1991.
13. Eriksson, K., "A domain independent integral expression for the crack extension force of a curved crack in three dimensions," Journal of the Mechanics and Physics of Solids, **50**, pp. 381-403, 2002.
14. Carter, B.J., Wawrzynek, P.A. and Ingraffea, A.R., "Automated 3-D crack growth simulation," International Journal for Numerical Methods in Engineering, **47**, 229-253, 2000.
15. Moës, N., Gravouil, A. and Belytschko, T., "Non-planar 3D crack growth by the extended finite element and level sets – Part I: Mechanical model," International Journal for Numerical Methods in Engineering, **53**, 2549-2568, 2002.
16. Gravouil, A., Moës, N. and Belytschko, T., "Non-planar 3D crack growth by the extended finite element and level sets – Part II: Level set update," International Journal for Numerical Methods in Engineering, **53**, 2569-2586, 2002.
17. Smith, C.W., Constantinescu, D.M. and Liu, C.T., "Stress intensities and crack growth in photoelastic motor grain models," Proceedings of the 2002 SEM Annual Conference& Exposition on Experimental and Applied Mechanics, Session 36, Experiments in Fatigue & Fracture, Paper 3, June 10-13, Milwaukee, Wisconsin, 2002.
18. Smith, C.W. and Kobayashi, A.S., "Experimental fracture mechanics," Chapter 20 of Handbook on Experimental Mechanics, 2nd Revised Ed., pp. 905-968, 1993.
19. Smith, C.W., Constantinescu, D.M. and Liu, C.T., "Crack shapes and stress intensities in a motor grain geometry," Proceedings of the 2002 International Conference on Computational Engineering & Sciences, Chapter 7, Paper No. 5, Technical Science Press, Irvine, Ca., 2002.
20. Marşavina, L. and Constantinescu, D.M., "Experimental and numerical crack growth in a special geometry," 21st International Congress of Theoretical and Applied Mechanics, paper SM9L_10864 in Section SM9 Fracture and crack mechanics (CD), August 15-21, 2004, Warsaw, Poland.
21. Wawrzynek, P.A. and Ingraffea, A.R., "Discrete Modeling of Crack Propagation: Theoretical Aspects and Implementation Issues in Two and Three Dimensions," Department of Structural Engineering, Report No. 91 – 5, Cornell University, 1991.
22. Erdogan, F. and Sih, G. C., "On the Crack Extension in Plates under Plane Loading and Transverse Shear," Journal of Basic Engineering, **85**, 519 – 525, 1963.